Chapter 22
Collective Dynamics of Pedestrians with No Fixed Destination

Takayuki Hiraoka, Takashi Shimada, and Nobuyasu Ito

Abstract In order to understand pedestrian dynamics, we construct a model of self-propelled disk particles interacting repulsively with no fixed destination. From molecular dynamics simulations, we find that the model exhibits collective motion and transition from a disordered to a polar-ordered, heterogenous state. Binary scattering study suggests that ordering originates from parallel alignment of particles' velocity after collision. The dependency of alignment tendency on the model parameter agrees well with the behavior of multiparticle systems. We verify that the model reproduces the actual pedestrian phenomena in a straight pathway. Although there is still a gap with empirical findings, especially in high densities, the result implies that pedestrian crowds can spontaneously build up a collective motion even in the situation where they have lost their destinations.

22.1 Introduction

From schooling of fish, flocking of birds, swarming of insects to migration of cells or bacteria, we often observe collective behaviors of biological organisms. One may presume that these fascinating pattern formation in nature is produced by sophisticated information processing mechanism specific to the species, by elaborate interaction between individuals, or by presence of a special individual who

T. Hiraoka (✉) • T. Shimada
Department of Applied Physics, Graduate School of Engineering, The University of Tokyo, 7-3-1 Hongo, Bunkyo-ku, Tokyo 113-8656, Japan

JST CREST, 4-1-8 Honcho, Kawaguchi, Saitama 332-0012, Japan
e-mail: hiraoka@serow.t.u-tokyo.ac.jp; shimada@ap.t.u-tokyo.ac.jp

N. Ito
Department of Applied Physics, Graduate School of Engineering, The University of Tokyo, 7-3-1 Hongo, Bunkyo-ku, Tokyo 113-8656, Japan

JST CREST, 4-1-8 Honcho, Kawaguchi, Saitama 332-0012, Japan

RIKEN AICS, 7-1-26, Minatojima-minami-machi, Chuo-ku, Kobe, Hyogo 650-0047, Japan
e-mail: ito@ap.t.u-tokyo.ac.jp

H. Takayasu et al. (eds.), *Proceedings of the International Conference on Social Modeling and Simulation, plus Econophysics Colloquium 2014*, Springer Proceedings in Complexity, DOI 10.1007/978-3-319-20591-5_22

takes leadership. However, recent studies on self-propelled particle systems revealed that collective motion could arise even in the absence of long-range communication, complex behavioral rules, and global leadership [1–3]. Furthermore, it has been shown that the non-equilibrium character enables the systems to develop long-range order and anomalously large density fluctuations, which are unusual in equilibrium systems [4–8]. Recent studies have found these features are shared not only by biological organisms but also by non-biological systems such as vibrated granular particles, in which explicit alignment with neighbors are absent [9].

One of the important research subject studied under the concept of the self-propelled particle is the pedestrian dynamics. We notice that there are characteristic patterns of crowds in streets, intersections, train stations, airport terminals, concert halls, sport stadiums, political demonstrations, etc. Such patterns in the urban environment spontaneously arise from individuals moving with their own destinations or intentions. Many microscopic models have been proposed to describe pedestrian movement. They can be categorized into two main types: cellular automata models [10, 11], in which time and space is discretized, have an advantage in computational cost, while force-based models, which is inspired by Newtonian mechanics, can simulate realistic trajectories [12, 13]. Excluded volume interaction and repulsion due to social psychological effect play an important role in both types of model.

In this proceedings we aim to establish a kinetic understanding towards the collective dynamics of self-propelled particle systems with repulsive interaction. In order to find out whether the crowd develops collective behavioral order, we construct a simple self-propelled particle model which assumes no constant destination nor explicit alignment interaction. We report the details of the model and the results obtained from the numerical simulations.

22.2 Model and Simulations

Among many pedestrian models that has been previously proposed, the social force model [12] is the one that has been widely recognized. It assumes that each pedestrian follows Newtonian equation of motion, which consist of the sum of self-driving force towards the destination and repulsive forces, namely the exponential "social force" from other pedestrians. In addition to the social force, another literature [14] introduces normal body force and tangential friction that describes physical contacts between people.

In order to construct a simple model and to clarify the physical meaning of crowd dynamics, we start with two assumptions:

- Pedestrians do not have constant destination.
- Pedestrians interact with linear elastic repulsive forces.

It may seem improbable that pedestrians have no destination on their way. However, they can in fact lose or abandon their destinations in extremely dense crowd. The

latter point also reflects highly dense conditions where excluded volume effect plays a pivotal role in crowd dynamics.

Let us consider N polar disk particles of equal radius a moving on a two-dimensional continuous surface. The polarity of each disk is defined by an unit vector $\hat{\mathbf{e}}(\psi_i) = \cos\psi_i\hat{\mathbf{x}} + \sin\psi_i\hat{\mathbf{y}}$. The equation of motion is given by

$$\frac{d\mathbf{v}_i}{dt} = \alpha\hat{\mathbf{e}}(\psi_i) - \beta\mathbf{v}_i + \sum_j \mathbf{f}_{ij}, \tag{22.1}$$

where $\mathbf{r}_i$ denotes the position of particle i, and the direction of their velocity is θ_i, i.e., $\mathbf{v}_i = v_i(\cos\theta_i\hat{\mathbf{x}} + \sin\theta_i\hat{\mathbf{y}})$.

Particle i drives itself with a self-propulsion force of constant magnitude α along its polarity axis while the velocity is damped by a drag force of coefficient β. The dynamics of the polarity is overdamped by a torque proportional to the angular deviation from the direction of the velocity, as

$$\frac{d\psi_i}{dt} = \gamma(\theta_i - \psi_i), \tag{22.2}$$

where γ is the damping coefficient.

We assume that the interaction between particles i and j is given by a steric repulsive force with a linear elasticity, i.e., $\mathbf{f}_{ij} = -k\left(2a - r_{ij}\right)(\mathbf{r}_i - \mathbf{r}_j)/r_{ij}$ if $r_{ij} = |\mathbf{r}_i - \mathbf{r}_j| < 2a$ and $\mathbf{f}_{ij} = 0$ otherwise. Note that the momentum is conserved by the interaction itself. Without loss of generality, we set length unit $2a = 1$ and time unit $\beta^{-1} = 1$ and obtain rescaled equations of motion. The model is then governed by three time scales: α^{-1} is the time for a free particle to travel its own diameter, γ^{-1} is the angular relaxation time of polarity, and $k^{-1/2}$ is the elastic time scale of collision.

The magnitude of self-propulsion force and elastic modulus are fixed as $\alpha = 1$ and $k = 100$, respectively. Under such choice of parameter values, particles penetrate their neighbors by at most $\sim 1\,\%$ of their diameter. Therefore the elasticity is large enough to avoid unrealistic situation where particles in contact pass through each other. Although the empirical value of elasticity of human body is not known, Helbing et al. [14] estimates it as $k = 1.2 \times 10^5\,\mathrm{kg\,s^{-2}}$. Given that the mass of a pedestrian is 80 kg and $\beta^{-1} \simeq 0.5$ s, the scaled elasticity will be $k \sim 10^2$, which is consistent with the above value.

22.3 Spontaneous Ordering with Periodic Boundary Conditions

We performed molecular dynamics simulations with $N = 10{,}000$ particles on a square plane of size L with periodic boundaries. Initial configurations are assigned randomly in terms of particles' position and their direction of polarity. The overlaps

between particles have been reduced by evolving the system only by the interaction forces for a sufficient time prior to each simulation. The two control parameters of the simulations are the angular damping coefficient γ and the packing fraction

$$\rho = \frac{\pi N a^2}{4L^2}. \tag{22.3}$$

In the region where damping is weak, the system exhibits polar ordering and clustering as shown in Fig. 22.1. To characterize the collective motion, we employ as the order parameter the global polarization

$$\phi = \frac{1}{N}\left|\sum_{i=1}^{N} \hat{\mathbf{e}}(\psi_i)\right|, \tag{22.4}$$

whose value is finite in the phase with polar order, and goes to zero in a globally disordered state.

For a fixed packing fraction, the growth of the order parameter is slow when damping coefficient is small ($\gamma \ll 1$). It is because each particle tends to keep its polarity to the same direction as given in the initial random state. As the damping parameter increases, the speed of polarity alignment becomes faster. However, increasing the damping parameter further slows down the development of the order. Above a certain value of γ, no collective motion takes place so that the system remains disordered and isotropic. Close to this phase boundary, the time until the system builds up a polar order exceeds the computationally feasible time, which makes us difficult to identify the exact transition point. Therefore, we carried out multiple (typically 16) runs with different initial configurations for each set of control parameters, ρ and γ, and categorized the corresponding point in the parameter space as polar-ordered phase if ϕ grows larger than 0.5 for at least one realization. Obtained phase diagram is shown in Fig. 22.2.

22.4 Binary Scattering Study

In this section, we give a simple explanation to understand the mechanism that underlies the characteristic ordering behavior shown in previous section. Let us limit our discussion only to the binary particle collision process [15]. Here we assume the system is dilute enough ($\rho \to 0$) so that only the uncorrelated, binary collisions take place, and both the velocity and the polarity are fully relaxed before each collision.

If the damping is weak, the polarities of two particles remain unchanged, so the directions of motion are temporally changed by the collision but eventually restored to the original direction. Here the relative angle between the velocities does not change before and after the collision. By contrast, if the damping is strong, the polarities rotates themselves quickly to align to the directions of motion, so the particles moves as if they have exchanged their momentum. Here again the absolute

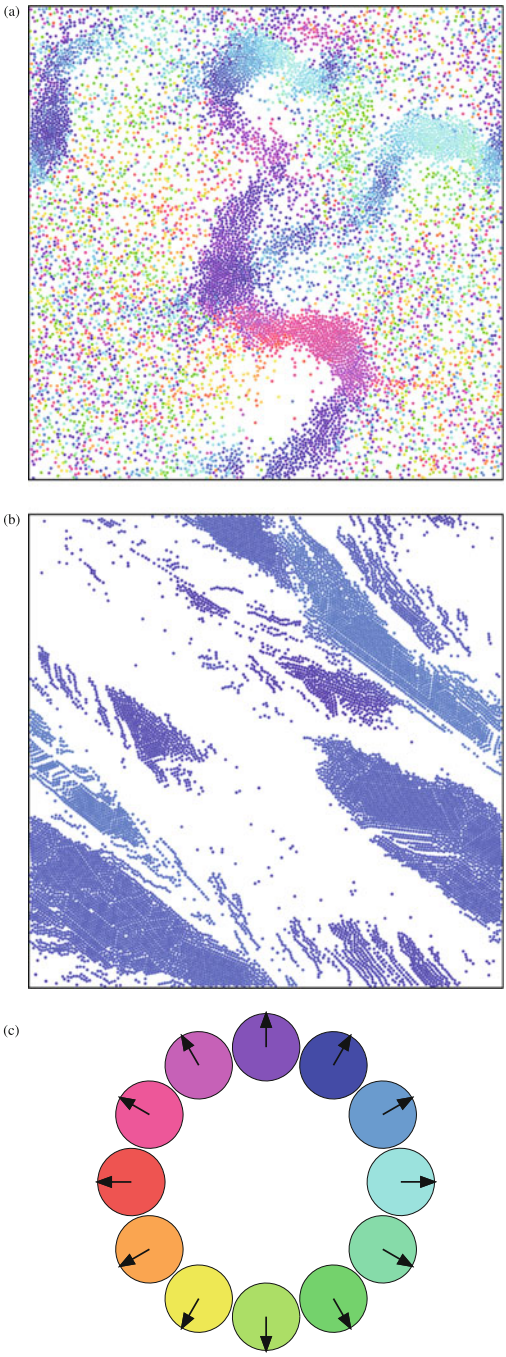

Fig. 22.1 Typical snapshots of a system in periodic boundary boxes (**a**) at onset of the collective motion, and (**b**) at fully ordered state. The packing fraction $\rho = 0.3$ and the damping parameter $\gamma = 20$. The *color* denote the polarity of each particle, as shown in (**c**)

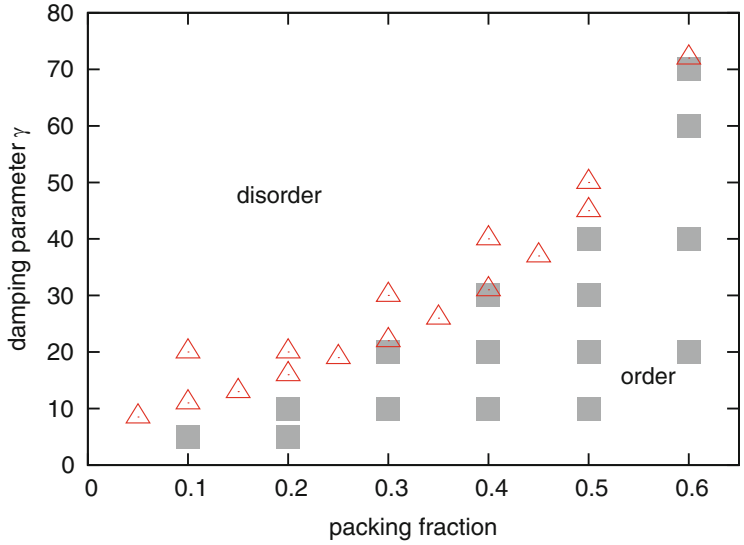

Fig. 22.2 The ρ-γ phase diagram obtained from molecular dynamics simulations. *Gray squares* denote states that polar order is observed and *red triangles* indicate the phase where the system remains disordered. We suppose that disordered phase stretches to the upper left domain, where we does not have numerical results yet

value of the relative angle is maintained. For an intermediate damping parameter, the motion of two bodies align parallel due to the competing effect of the collision and the subsequent angular damping.

Numerical results support this qualitative conjecture. Consider a binary scattering process between particle i and j. Since we assume the rotational invariance, the geometry of the moment of contact is fully specified by two scalar parameters: the impact parameter $b_{ij} = \sqrt{r_{ij}^2 - \mathbf{r}_{ij} \cdot (\mathbf{v}_i - \mathbf{v}_j)/v_{ij}} \in [0, 1]$, where $v_{ij} = |\mathbf{v}_i - \mathbf{v}_j|$ and the relative angle $\theta_{ij} = |\theta_i - \theta_j| \in [0, \pi]$, as shown in Fig. 22.3. The impact parameter shows the perpendicular offset of the two bodies' center of mass from head on collision. If $b_{ij} = 0$ the collision is head on whereas it is a miss if $b_{ij} > 1$.

Instantaneous alignment of the two particles are characterized by two-particle polarization

$$\phi^{(2)} = \frac{1}{2} \left| \hat{\mathbf{e}}(\psi_i) + \hat{\mathbf{e}}(\psi_j) \right|, \tag{22.5}$$

which corresponds to the global polarization [Eq. (22.4)] with $N = 2$. We measure the two-particle polarization $\phi_{\text{out}}^{(2)}$ at an adequate time for the polarities and the velocities to relax after the collision, and compare it to the polarization $\phi_{\text{in}}^{(2)}$ before the collision. The increment,

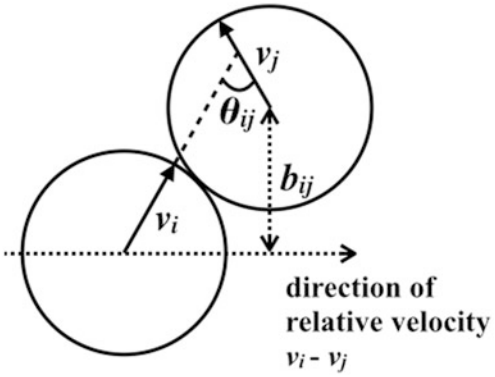

Fig. 22.3 Schematic view of collision geometry. The geometry is defined by the relative angle θ_{ij} and impact parameter b_{ij}. We assume that the two particles are fully relaxed in terms of velocity and polarity before each collision, therefore $\mathbf{v}_i/|\mathbf{v}_i| = \hat{\mathbf{e}}(\psi_i)$

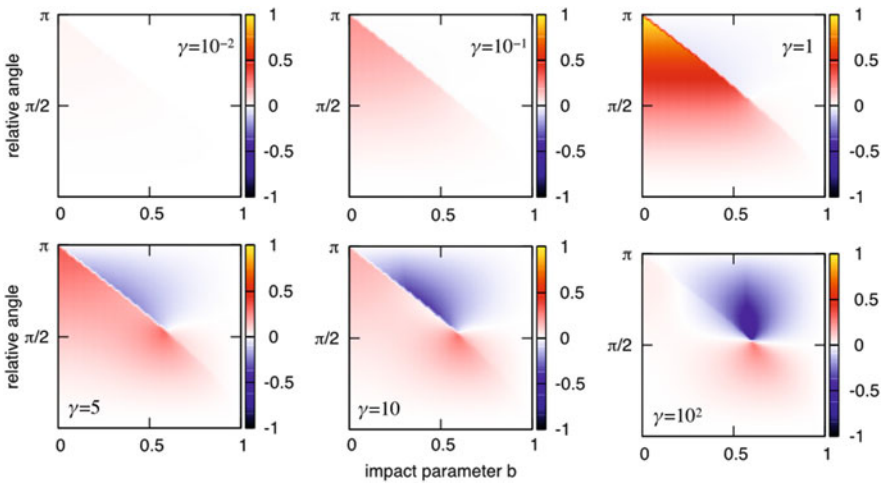

Fig. 22.4 The two-particle polarization increment $\Delta\phi^{(2)}$ as a function of relative angle θ_{ij} and impact parameter b_{ij}. γ is varied as denoted in the figure. For the collision geometry in the *red* region, the collision makes particles align to each other ($\Delta\phi^{(2)}(b,\theta) > 0$), while in the *blue* region it result in antiparallel alignment ($\Delta\phi^{(2)}(b,\theta) < 0$)

$$\Delta\phi^{(2)} = \phi^{(2)}_{\text{out}} - \phi^{(2)}_{\text{in}}, \tag{22.6}$$

indicates the magnitude of parallel alignment caused by the binary scattering process. Figure 22.4 depicts $\Delta\phi^{(2)}$ as a function of the collision geometry (b_{ij}, θ_{ij}).

Assuming that the multiparticle system is homogenous and isotropic, the probability that the two particles collide in the relative angle of θ_{ij} is proportional to v_{ij} and that impact parameters b will be equally distributed. Therefore we can obtain

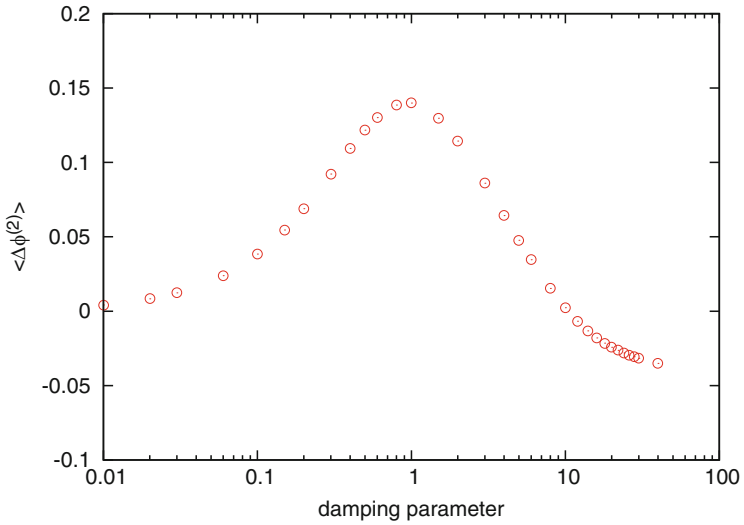

Fig. 22.5 Average alignment tendency integrated over all collision geometries, as a function of the damping parameter γ. Note that for large values of γ, the tendency drops to negative values

average tendency to align parallel for a specific value of γ by estimating the expected value with an integration weight of "scattering cross section"

$$\langle \Delta\phi^{(2)} \rangle = \frac{1}{C} \int \mathrm{d}b \int \mathrm{d}\theta_{ij} \left| \sin\left(\frac{\theta_{ij}}{2}\right) \right| \Delta\phi^{(2)}(b_{ij}, \theta_{ij}), \tag{22.7}$$

where C is a normalization constant.

The result shown in Fig. 22.5 indicates that the alignment tendency hits its peak at $\gamma \sim 1$. For $\gamma \to 0$, which corresponds to the regime where angular relaxation is slow, $\langle \Delta\phi^{(2)} \rangle$ goes to zero. For large γ, namely $\gamma \to \infty$, $\langle \Delta\phi^{(2)} \rangle$ has a negative value. This picture have two consistency with the result obtained from the multiparticle simulations; (1) The ordering in many-body system is the fastest in the parameter region that maximize the value of $\langle \Delta\phi^{(2)} \rangle$; (2) The transition in the dilute system occurs at $\gamma \sim 10$, where $\langle \Delta\phi^{(2)} \rangle$ changes its sign. These points imply that at least for the dilute limit $\rho \to 0$, the onset of collective motion arise from the repetition of binary collision process.

22.5 Flow in a Pipe

In order to validate the correspondence of the model with actual pedestrian phenomena, we performed multiparticle simulations in a "pipe", i.e., a rectangular area with periodic boundaries in the longitudinal direction and fixed repulsive

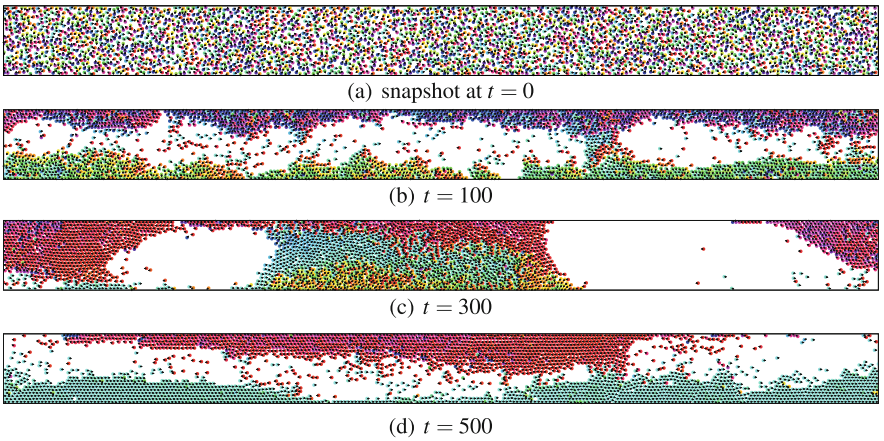

Fig. 22.6 Snapshots of the simulations carried out under "pipe" condition. The system consist of $N = 3200$ particles and is periodic for x-direction while bounded by elastic slipping walls for y-direction. The width of the pipe is 20.0, $\rho = 0.5$, $\gamma = 0.01$. At $t = 300$, three-lane structure is observed. (**a**) snapshot at $t = 0$, (**b**) $t = 100$, (**c**) $t = 300$, (**d**) $t = 500$

boundaries in the lateral direction. The interaction between the particles and the repulsive boundaries is assumed to be similar to the particle-particle interaction, that is, the interaction potential is elastic and frictionless. Starting from random initial condition, the system develops into two lanes of particle flow moving in opposite directions for certain sets of parameters (Fig. 22.6). Three-lane structure is also observed in a transient state. These results indicate that the model can reproduce the lane formation, which is one of the basic self-organization phenomena observed in pedestrian crowd [12]. The stability of lane structures and their dependency to the width of the pipe are subject of future investigation.

22.6 Summary and Discussion

In order to close the gap between theory on self-propelled particles and pedestrian dynamics study, we proposed a self-propelled particle model with repulsive interaction, and examined its collective behavior through many-body simulations. Binary scattering studies demonstrate the microscopic mechanism underlying the transition from a disordered to a polar-ordered phase.

Our model assumes that the collision process itself is elastic, i.e., no dissipation is taken into account. Nevertheless, the effective inelasticity introduced by the angular damping allows the formation of clusters, or "flocks," similar to that of granular gases. Of course, this argument is not exact because the many-body correlation cannot be ignored once local clusters are formed. Still, it provides a qualitative and,

to some extent, quantitative explanation. We look forward to a further discussion on many-body effect and on cluster-cluster interaction.

The conventional social force model [12] assumes that each pedestrian experiences the social force from other pedestrians in his/her eyesight, which is described as an exponentially decaying repulsion. We expect that any isotropic, short-ranged repulsive potential, including exponential one, would not deviate the overall property of the system from the results we obtained with linear elastic repulsion. On the other hand, introduction of anisotropic potential that reflects the fact that pedestrians react stronger to the situation in front of them is not clear and yet to be discovered.

It is known that high crowd density leads to a turbulent movement of pedestrians and increases the risk of crowd disaster [16]. In spite of social demands to prevent such accidents from occurring and from spreading, their mechanism is yet to be uncovered, since experiments cannot be carried out due to ethical reasons, and observational data are hardly available. Previous pedestrian models assume that every agent is aware of its own destination and keeps driving itself until it reaches to that point. However, there are circumstances when pedestrians are not so conscious of where they are heading to. In fact we scanned the footage from the crowd disaster happened in Germany in 2010 and found that people sometimes behave as if they have lost or abandoned their initial destination in extremely dense crowd.

To this end, we verified that our model, which has no fixed destination, could display bidirectional lanes similar to what is observed in pedestrian flows in a straight pathway. Here, the damping parameter γ in the model can be regarded as the quickness of one's reaction to a contact with neighbor walkers. However, the phase diagram shows that in higher density, the order develops for a broader range of the parameter, which does not meet with the empirical facts. By improving the model we expect that our result can lead to a further understanding on the mechanism of crowd disasters.

References

1. Vicsek T, Czirók A, Ben-Jacob E, Cohen I, Shochet O (1995) Phys Rev Lett 75:1226
2. Czirók A, Stanley HE, Vicsek T (1997) J Phys A Math Gen 30:1375
3. Grégoire G, Chaté H, Tu Y (2003) Phys D Nonlinear Phenom 181:157
4. Toner J, Tu Y (1995) Phys Rev Lett 75:4326
5. Toner J, Tu Y (1998) Phys Rev E 58:4828
6. Simha RA, Ramaswamy S (2002) Phys Rev Lett 89:058101
7. Ramaswamy S, Simha RA, Toner J (2003) Europhys Lett 62:196
8. Chaté H, Ginelli F, Montagne R (2006) Phys Rev Lett 96:180602
9. Narayan V, Ramaswamy S, Menon N (2007) Science 317:105
10. Burstedde C, Klauck K, Schadschneider A, Zittartz J (2001) Physica A 295:507

11. Kirchner A, Nishinari K, Schadschneider A (2003) Phys Rev E 67:056122
12. Helbing D, Molnár P (1995) Phys Rev E 51:4282
13. Yu WJ, Chen R, Dong LY, Dai SQ (2005) Phys Rev E 72:026112
14. Helbing D, Farkas I, Vicsek T (2000) Nature 407:487
15. Hanke T, Weber CA, Frey E (2013) Phys Rev E 88:052309
16. Helbing D, Johansson A, Al-Abideen H (2007) Phys Rev E 75:046109